Iterative Slepian Cancellation with Track Before Detect In Radar Processing String

Dr. Lisa Osadciw, Dr. Aaron Skewes[1], Samuel Stone[1], Charles J Roberts[1], Alexander Thornton[1], Dominic DiPuma[1], Harrison Stanton[1], Nguyen Nguyen[3], Coleman Delude[2], Dr. Anthony Murray[4], Dr. Mark Davenport[2], Dr. Justin Romberg[2]

[1]Lockheed Martin RMS, Syracuse, NY
[2]Georgia Technical Institute of Technology, Atlanta, GA
[3]Lockheed Martin RMS, Moorestown, NJ
[4]Lockheed Martin AL, Cherry Hill, NJ

lisa.a.osadciw@lmco.com

***Abstract*— This project is part of DARPA Beyond Linear Processing (BLiP) that proposes integrating compressive sensing techniques, artificial intelligence, machine learning, and track-before-detect algorithms into a comprehensive processing string for radar systems. This effort focuses on the control, interfaces, and impact each algorithm has on the system's processing. The challenges result from designing the algorithms to work together cohesively to minimize signal loss that has been traditionally accepted within existing radar systems. The objective is the ability to reduce the antenna or front-end hardware, which is the prime cost driver in fielding radars today. Integrating processing from recent signal processing advances is a cost-effective alternative to improve a radar's sensitivity, accuracy, and volume coverage.**

Keywords—Space-Time-Adaptive-Processing (STAP), Adaptive Signal Processing, Direct Prolate Spherical Sequence (DPSS), Slepian Transform, Track-Before-Detect Tracking, Convolutional Neural Networks (CNNs),

I. Introduction

Since the algorithm research performed in the 1960s-1970s, the focus in radar has been to advance the hardware in order to improve performance. This approach is based on assumptions that made sense for the processing capabilities until recently. Since then, computer hardware capabilities as well as the mission requirements have progressed so that these assumptions and traditional processing limitations require rethinking. This program's effort is to integrate a new processing architecture that uses compressive sensing, AI/ML to enhance Space-Time Adaptive Processing (STAP), AI/ML enhanced detection, and introduces a new track before detect approach as nonlinear processing elements. During the program, the team will plan to demonstrate a performance enhancement estimated at 15-20 dB. This loss reduction directly shrinks the system's power generation needs and array size. This impacts the radar system's mobility and cost supporting other radars and sensors overlapping in coverage presenting a more accurate picture of the space. In this paper, we provide an overview of the Lockheed Martin – Georgia Institute of Technology team's Beyond Linear Processing string architecture, including random pulse repetition rate (PRF) processing, advanced compression, Knowledge Aided High Dynamic Range Space Time Adaptive Processing (KA-HDR STAP), Object Amplification Test (OAT), Track-Before-Detect (TBD) Tracker, and an AI/ML approach to estimating and managing environmental assessment. This paper describes this team's approach, a culmination of advancements in radar signal processing.

II. Architecture Overview

The architecture focuses on reducing interference from neighboring RF sources that exist in a dense spectrum environment. The random PRF results in irregularly spaced pulses and requires aligning to create a data cube that STAP can use to coherently cancel clutter and/or interference in time and Doppler. The alignment depends on the assumption that returns are first, second, or N^{th} time around. This architecture focuses on each assumption using a separate string in parallel. KA HDR STAP is applied to these In-phase and Quadrature (IQ) data cubes associated with each specific time around assumption [3] [6]. An iterative suppression technique from compressive sensing work in [5] reduces the interference further. The last technique prior to tracking is OAT, which is a U-net trained to recognize the various compressed pulses in a wide variety of situations and varying signal-to-noise ratio powers. Finally, the TBD tracker receives all the range-Doppler maps following the iterative suppression for the selected time around returns processed associated with confidence levels from OAT. The TBD tracker integrates this information from the suppression outputs with OAT's confidence in whether it is a unique target return or not, which assists in reducing the processing for track birthing. The team has an IQ data simulator to robustly train and test the string for a specific radar. This string is illustrated in Figure 1. A containerized testing strategy also supports playback of recorded radar data.

III. Containerized Testing Strategy

A. Open and flexible architecture

The Wideband RF Adaptive, Intelligent Target Hunting Network (WRAITHNet) testbed architecture meets OCS standards [14] including containerized applications, which

This work is supported under DARPA BLiP Contract No. FA2385-23-C-001. This work has been reviewed and is approved for publication with DISTRIBUTION STATEMENT A. Approved for public release: distribution is unlimited. The views presented in the paper are not necessarily those shared by DARPA.

enables fast and cost-efficient integration of these new capabilities. This is achieved by defining common standards, interfaces and best practices for system and component development. There are three primary categories of interfaces identified for this project: 1) streaming IQ data interface; 2) high-speed (e.g. real time) message bus and 3) low-speed message bus following OMS as described in [15].

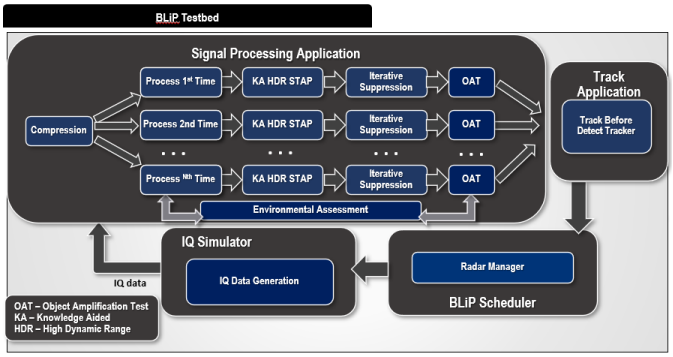

Figure 1: A diagram of the DARPA BLiP testbed employing containerized integration. Each large block (e.g. Signal Processing Application) represents a skill comprised of a collection of services (small blocks). The arrows follow the general signaling flow and in practice will connect containers via data adapters.

B. DARPA BLiP Testbed

A diagram of the DARPA BLiP testbed is a skill in Figure 1. There are two primary applications, or services, within the skill's scheduler. In addition to the IQ Simulator provides data similar to that received from the radar's front end. Each service is comprised of digital payloads or libraries listed below. The objective of this approach is to provide a more flexible integration approach that will really assist in efforts to integrate new string processing such as the services in BLiP. The service interfaces are controlled so that the teams can generate or receive data in the proper format sooner and iterate for testing and analytical purposes more frequently. The IQ simulator skill is another enabler of this testing approach. Test and iterate often. As shown below, some services consist of a single digital payload, which depends on the design of the functionality.

BLiP Skill

1. Signal Processing Application Service:
    a. Compression Digital Payload
    b. Process Nth Time Digital Payload
    c. KA HDR STAP Digital Payload
    d. Interference Suppression Digital Payload
    e. OAT Digital Payload
2. Track Application Service
    a. Track before Detect (TBD) tracker Digital Payload
3. BLiP Scheduler Service
    a. Radar Manager Digital Payload

IV. Key Characteristics of the New Processing Strategies

A. Compression and Nth Time Processing

The objective of these two processing blocks is to set up the data for the remainder of the post processing. The National Oceanic Atmospheric Administration Phased Array Radar (NOAA PAR) system in Norman, Oklahoma, is a radar testbed well suited for testing these algorithms and pulse compresses the data prior to sending it from the antenna or front end. Its typical array beam patterns are shown for simulated data in Figure 2.

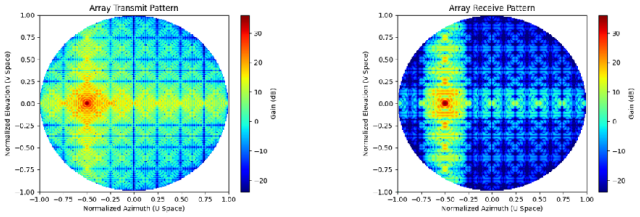

a. Transmit Pattern *b. Receive Pattern*

Figure 2: Simulated Array Patterns with No Noise representative of NOAA PAR, Norman, Oklahoma, (a) Transmit Pattern (b) Receive Pattern.

The automatic pulse compression is removed by convolving the inverse of the weights used on pulse compression for its NLFM waveform. This string will test compression using Slepian weights to reduce signal losses that typically occur. With additional interference reduction in the time sidelobes accomplished by the Interference Suppression and OAT techniques, any weighting needed to reduce time sidelobes, especially for an LFM waveform, can be removed. There is some weighting present to protect the hardware and that will remain. The pulses are then aligned properly assuming the reflection is from a particular pulse. This allows time to be referenced properly as well as any phase adjustments needed for holes in the receive window. The output is an IQ data cube to the STAP process based on each (up to *N*) of the target-pulse reflection association assumptions.

B. KA HDR STAP for ground-based air-surveilance radar

While ground-based air-surveillance radars are less hindered by ground clutter than airborne radars, radars such as NOAA PAR operate near the resonant frequencies of Water and Hydrogen in order to detect weather. STAP is being investigated for both ground and weather clutter rejection as well as for interference mitigation in the crowded spectrum and later transitions to airborne applications. For this ground application, however, airborne target detection within weather clutter is of interest. Wind, rain, and snow sources of clutter make it challenging to detect low and slow targets, such as an UAS. An advanced STAP technique using Slepian basis functions will be leveraged to remove weather and wind-blow clutter while significantly reducing STAP's characteristic signal processing losses [3].

This effort will focus on maturing the KA HDR STAP processing. The KA HDR STAP algorithm from [3] is summarized and illustrated in Figure 3. The algorithm is similar to eigenvalue decomposition in STAP except the Slepian

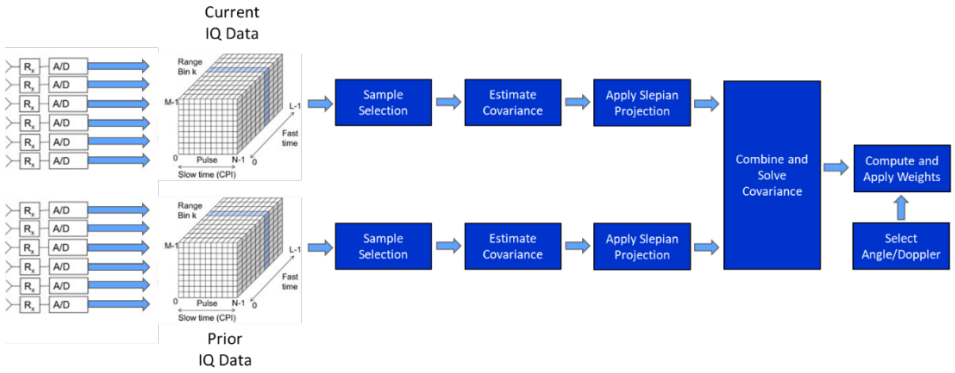

Figure 3 Architecture of the KA-HDR-STAP algorithm with Primary Processing Steps

transform is used in place of PCA. This results in both a real time algorithm if using the Fast Slepian Transform, a wideband technique, and significantly reduces signal processing losses on the order of 3 dB while improving cancellation for spikey heterogeneous clutter. The technique is further improved by using covariance matrices from sample sets with similar clutter amplitude distributions. As shown in Figure 4, the clutter cancellation ratio (CCR) is improved and stabilizes more quickly using additional sample sets. Environmental Assessment is the processing that estimates and maintains histories of the covariance estimates across the surveillance volume. This is described in the next session.

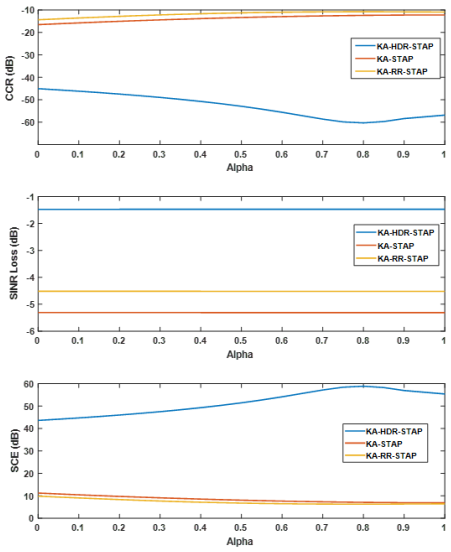

Figure 4: Performance Advantages for KA HDR STAP Using Additional Covariance Matrix Estimates Especially in the Clutter Cancellation Area While Other Techniques Only Benefit Slightly.

C. Environment Assessment

For environmental assessment, the objective is to segment the clutter reflection amplitudes based on their statistics and statistical deviation from Gaussian clutter [2][12]. At the high level, the process is described in Figure 5.

Figure 5: Functional flowchart of the environmental assessment process.

According to Figure 1, the raw IQ data is processed by environmental assessment after pulse compression. This prevents any smearing of a clutter's response into neighboring range bins for the S-band frequencies. Since the interference and clutter may be in the sidelobes, training samples should be drawn from multiple receive channels and PRIs. In NOAA PAR, the receive channels are already sub-arrayed and steered close to the region of interest. The vector is processed using a sliding window of 200 through 400 fast-time samples across *PRI*s and channels. The training sample sets are used to estimate the statistical shape and scale (ν and α respectively) of clutter or interference. Eventually, the estimated weights will be applied to the samples within the index range corresponding to these training samples. To calculate shape and scale, one must estimate and use a few non-central moments given by

$$\mu_k = \frac{1}{M}\sum_{i=0}^{M-1} x_i^k, \tag{1}$$

$$\nu = \frac{4-\frac{\mu_4}{\mu_2^2}}{\frac{\mu_4}{\mu_2^2}-2}, \tag{2}$$

$$\alpha = \frac{\mu_1}{\sqrt{\pi}}\frac{\Gamma(\nu+1)}{\Gamma(\nu+1.5)}. \tag{3}$$

Currently, the team is using the product of skew and kurtosis, which can be derived from shape and scale, to distinguish between segments of heterogeneous, K-distributed clutter [13]. Then clustering is used to determine boundaries between distributions and the pairing between like distributions for training purposes. This approach is an enhancement on a body of earlier work performed in 1990s-2010s studying clutter distributions.

A simple example of this method is shown using simulated clutter and varying the distributions in range. The impact of range on the amplitude is added by incorporating the inverse 4th power of the simulated range values. Thermal noise is added as white gaussian noise to achieve an average of 20 dB

CNR. As clutter disappears, the noise becomes the dominating distribution. In Figure 6, an example of six clutter regions is illustrated. The impact of range on clutter power is clearly evident preventing the use of the first two moments, mean and variance, to distinguish between the clutter types. The team has aligned the distribution boundaries with clear geographical features using real-world data. Also, there are clear spikes evident around range cells 2000 and 5000 in Figure 6. This occurs for major feature differences. As shown in Figure 1, the resulting information from this clutter segmentation is used by OAT and the TBD Tracker.

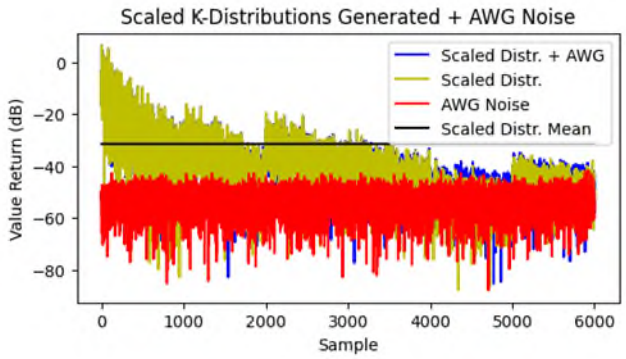

(a)

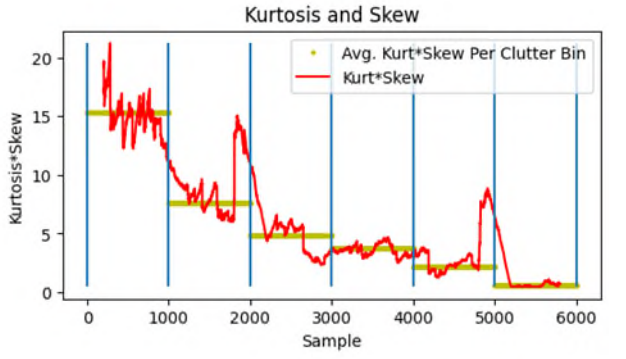

(b)

*Figure 6: (a)Six Pure K-distributions scaled for a radar range of 0.5-5km with AWG noise 20dB below the mean clutter value. (b) Resulting Kurtosis*Skew values plotted along the sample axis with vertical lines showing the transitions between K-distributions.*

D. Object Amplification Test (OAT)

The OAT has resulted from transitioning recent successes in AI/ML-based medical image recognition to radar signal processing. Medical image recognition solves similar problems that are addressed by radar signal processing: both domains attempt to detect, locate, and classify objects in a sparse environment using compressed energy. Errors either as false detections or misses in either field can lead to serious consequences. One approach with documented success in the medical field is a unique convolutional neural network architecture [11], which down-samples and then up-samples its input with aggressive use of skip connections, as shown in Figure 7.

Lockheed Martin (LM)'s prior internal research on applying the U-Net architecture to pulse-compressed radar I/Q data resulted in a radar detector which produced gains of approximately 3 dB versus a cell averaging – constant false alarm (CA-CFAR) detector. For BLiP, the LM RMS team will remove the U-Net's detection layer and simply provide the OAT's likelihood outputs along with additional data to inform the RFS TBD tracker's probability estimates.

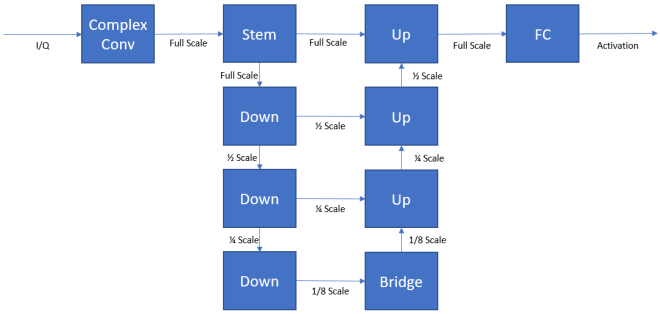

Figure 7: High-Level U-Net Architecture

E. Track-Before-Detect Tracker

Multi-target tracking approaches typically rely on a detector to reduce the quantity of sensor data that the tracker needs to process. However, using a detector also sacrifices valuable information that is especially important in low-SNR scenarios where detector performance suffers. WRAITHNet uses a random finite set track-before-detect (RFS-TBD) tracker known as the G-LMB-GOM filter [17]. This enables track updates to be made directly on the range-Doppler maps constructed by OAT, improving performance on low-SNR targets.

When target birth locations are not known a priori or cued by an outside source, multi-target trackers must initiate new tracks solely from the measurements—a process known as measurement adaptive birth. Adaptive birth procedures usually require a detector[16][17][18], so likelihood data from the OAT processing provides more fidelity than a typical detector for track initiation. Once a track is initiated, all future updates will use the range-Doppler maps.

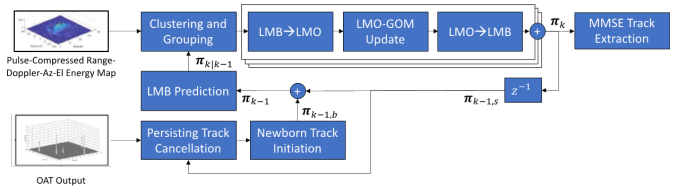

Figure 8: Block diagram of the G-LMB-GOM filter integration into the WRAITHNet String.

However, OAT data allows a graceful approach to scaling back track hypotheses if loading becomes an issue. Hypotheses may be prioritized using the information from OAT to designate stronger beliefs in a target's return.

F. Iterative Suppression

Recent work [1][5] has shown that the Fast Slepian transform [4] can be used to efficiently separate, remove interference, and beamform signals and relax Nyquist sampling requirements over traditional approaches. This works because an array effectively non-uniformly oversamples the signal if one considers both the time and spatial domain. The Fast Slepian

approach to iterative interference cancellation during beamforming can be extended to the doppler and time domain as needed. This section provides a deeper dive into some of the key approaches used in the design.

G. Fast Slepian Transform

While the Slepian basis, or Discrete Prolate Spheroidal Sequences, and Multi-taper Spectral Estimation have been well known since its introduction [7][8][9], it has only recently been practical for real-time radar systems with the introduction of a fast approximation for the Slepian transform [4].

The Fast Slepian Transform projects the major Slepian basis elements for a given signal bandwidth and sampling rate onto DFT functions. This enables the continued use of an efficient FFT to be used in Slepian subspace filtering and dimension reduction methods [1]. This results in a more practical implementation of the Slepian transform. For a signal length of J samples, the FST computational complexity is $O(J \log J \log \frac{1}{\epsilon})$, which utilizes an error tolerance parameter, ε. This conveniently controls errors in our approximation of the ideal Slepian basis (5). The FFT has a known computational complexity, $O(J \log J)$. Thus, applications requiring less approximation error require a less complex Fast Slepian Transform (FST). The FST is significantly faster than with the exact Slepian Transform of $O(W J^2)$, where the normalized bandwidth for the signal is

$$W = \frac{B}{f_s}. \tag{4}$$

The digitization is set by, W, based on the sampling frequency, f_s, and signal source bandwidth, B. The JxJ discrete prolate spheroidal matrix with subspace filtering and dimensionality reduction is derived from

$$\Gamma_K[m,n] := \frac{sin2\pi W(m-n)}{\pi(m-n)} \tag{5}$$

for all $m, n \in \{0,1,\dots,J-1\}$. Then we approximate, Γ_K, using

$$\boldsymbol{\Gamma}_K = \boldsymbol{F}_K \boldsymbol{F}^*{}_K + \boldsymbol{L}_1 \boldsymbol{L}^*{}_2 + \boldsymbol{E}_F, \tag{6}$$

where $\boldsymbol{F}_K$ is a subset of DFT vectors corresponding to the lower frequencies, L_1 and $\boldsymbol{L}_2$ matrices of $O(J \log \frac{1}{\epsilon})$ and E_F giving an error of $\|E_F\| \leq \epsilon$ [4].

The fast Slepian transform, of complexity $O(N \log N \log \frac{1}{\epsilon})$, enables fast computation for applications of non-adaptive beamforming, doppler filtering, and pulse compression. Fast Multi-taper spectral estimation, of complexity $O(KN \log N)$ for K tapers, enables real time signal separation using angular, Doppler, or time spreading of the sources [10].

H. Beamforming

A diagonal modulation matrix [5],

$$\boldsymbol{E}_{\boldsymbol{fc},\boldsymbol{\tau}}[m,m] = e^{-j2\pi f_c \tau_m}, \tag{7}$$

is formed using the time delays estimated at each antenna element or sub-array center computed by the projection of the center positions, $\boldsymbol{z_m}$, on the steering vector. The time delays are

$$\boldsymbol{\tau_m} = \boldsymbol{z_m^T s_\phi}/c. \tag{8}$$

Since we can approximate the signal using the first K modulated Slepian vectors, where K is determined by the bandwidth of the signal, $\mathbf{W}$, and the width of the temporal window, $\boldsymbol{T} = max(\tau) - \min(\tau)$, and an oversampling correction $\mathbf{L}$ as $K = \lceil 2WT \rceil + L$. We normalize the lags in (8) and use the first K Slepian basis sequences creating a non-uniform, $\boldsymbol{V_{nu}}$, and Nyquist, $\boldsymbol{V_{nyq}}$, sampled matrices. Slepian beamformed signal y becomes the Slepian weighted and summed signal, x, computed by

$$\boldsymbol{\psi^H} = \boldsymbol{V_{nyq}}(\boldsymbol{V_{nu}^H V_{nu}} + \boldsymbol{\sigma^2 I})^{-1} \boldsymbol{V_{nu}^H E_{f_c,\tau}^H} \tag{9}$$

and

$$\boldsymbol{y} = \boldsymbol{\psi^H x}. \tag{10}$$

This results in a non-adaptive Slepian beamformer or focuses energy without cancelling interference for broadband signals. The Slepian beamformer for a simulated wideband signal compared to a traditional narrowband beamformer applied to a 32 element uniform linear array is in Figure 9.

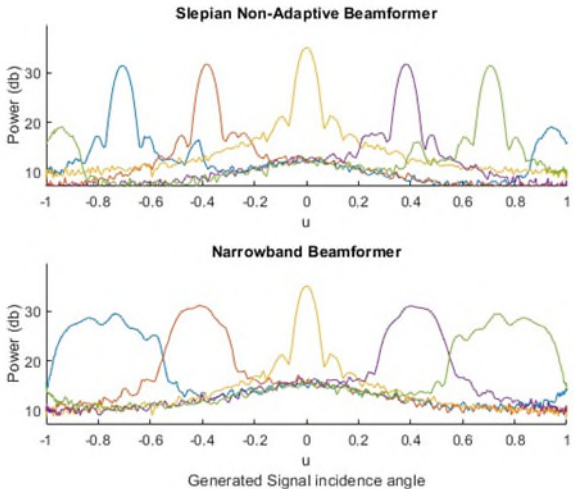

Figure 9 Non-adaptive Slepian vs Narrowband beamformer for simulated wideband signal, 20GHz center frequency and 5000MHz bandwidth

The performance of the Slepian beamformer demonstrates less degradation especially in beam broadening as a result of electronic steering. There is only signal loss due to the reduced antenna surface facing the target. Figure 10 shows the results of the Slepian and traditional beamformers processing in narrowband with narrowband signals.

I. *Iterative Interference*

The team will add interference cancellation with this Slepian processing in a variety of dimensions (e.g., angle, range, and Doppler). In (9), it is assumed that the bandwidth is known and centered around zero Hz with the array steered broadside. Practically, the beamforming, pulse compression, and additional Doppler filtering may be extended to remove a signal isolated from the target by estimating the location of the interference in one of these dimensions through an Orthogonal Matching Pursuit approach [5].

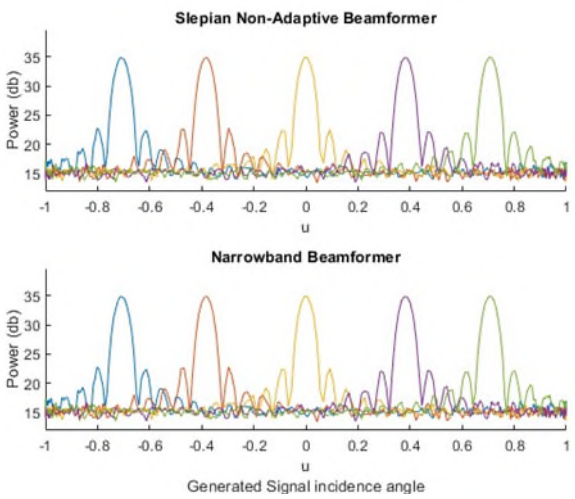

Figure 10 Non-adaptive Slepian vs Narrowband beamformer for simulated narrowband signal, 3GHz center frequency and 8MHz bandwidth

At the start of each iteration, a multi-tapered spectral estimate, S_f, is computed over a fine grid across the domain of interest for the residual, initialized with the input signal, x. From this, the Slepian basis for the largest remaining source, $\boldsymbol{\Psi}_1$, is computed from a refined range and center. This basis for the largest remaining signal is added to appended to a Slepian basis dictionary $\boldsymbol{\Psi}^{(i)} = [\boldsymbol{\Psi}^{(i-1)} \quad \boldsymbol{\Psi}_1]$. The signal is reconstructed from this dictionary as

$$\hat{\boldsymbol{x}} = \boldsymbol{\Psi}(\boldsymbol{\Psi}^H\boldsymbol{\Psi} + \sigma^2\boldsymbol{I})^{-1}\boldsymbol{\Psi}^H\boldsymbol{y}. \tag{11}$$

Then, the residual is computed as the difference between the original signal and the reconstruction of an isolated source by

$$\boldsymbol{r} = \boldsymbol{y} - \hat{\boldsymbol{x}}. \tag{12}$$

[5] provides more details on the algorithm and cases for a partially observed signal.

V. Summary and Plans Forward

This effort will result in a full radar processing string with the maturation of a variety of new techniques that have emerged from compressive sensing, artificial intelligence, and machine learning over the last decade. The advantages of these new techniques will be quantized and highlighted using NOAA PAR in Norman, Oklahoma, under DARPA BLiP.

References

[1] C. DeLude, S. Karnik, M. Davenport, and J. Romberg, "Broadband Beamforming via Linear Embedding." arXiv, Jun. 14, 2022. Accessed: Apr. 12, 2023. [Online]. Available: http://arxiv.org/abs/2206.07143

[2] L. A. Osadciw and J. F. Slocum, "Clutter processing using K-distributions for digital radars with increased sensitivity," in Proceedings of the 2002 IEEE Radar Conference (IEEE Cat. No.02CH37322), Apr. 2002, pp. 237–242. doi: 10.1109/NRC.2002.999725.

[3] L. Osadciw and D. Hebert, "Enhancing Space-Time Adaptive Processing Through the Slepian Transform 1," in 2021 IEEE Radar Conference (RadarConf21), Atlanta, GA, USA: IEEE, May 2021, pp. 1–6. doi: 10.1109/RadarConf2147009.2021.9455297.

[4] S. Karnik, Z. Zhu, M. B. Wakin, J. K. Romberg, and M. A. Davenport, "Fast computations for approximation and compression in Slepian spaces," in 2016 IEEE Global Conference on Signal and Information Processing (GlobalSIP), Washington DC, DC, USA: IEEE, Dec. 2016, pp. 1359–1363. doi: 10.1109/GlobalSIP.2016.7906063.

[5] C. DeLude, R. S. Srinivasa, S. Karnik, C. Hood, M. A. Davenport, and J. Romberg, "Iterative Broadband Source Localization," IEEE J. Sel. Areas Inf. Theory, vol. 4, pp. 453–469, 2023, doi: 10.1109/JSAIT.2023.3317094.

[6] X. Zhu, J. Li, and P. Stoica, "Knowledge-Aided Space-Time Adaptive Processing," IEEE Trans. Aerosp. Electron. Syst., vol. 47, no. 2, pp. 1325–1336, Apr. 2011, doi: 10.1109/TAES.2011.5751261.

[7] D. Slepian and H. O. Pollak, "Prolate Spheroidal Wave Functions, Fourier Analysis and Uncertainty - I," Bell System Technical Journal, vol. 40, no. 1, pp. 43–63, Jan. 1961, doi: 10.1002/j.1538-7305.1961.tb03976.x.

[8] D. Slepian, "Prolate Spheroidal Wave Functions, Fourier Analysis and Uncertainty - IV: Extensions to Many Dimensions; Generalized Prolate Spheroidal Functions," Bell System Technical Journal, vol. 43, no. 6, pp. 3009–3057, Nov. 1964, doi: 10.1002/j.1538-7305.1964.tb01037.x.

[9] D. Slepian, "Prolate Spheroidal Wave Functions, Fourier Analysis, and Uncertainty-V: The Discrete Case," Bell System Technical Journal, vol. 57, no. 5, pp. 1371–1430, May 1978, doi: 10.1002/j.1538-7305.1978.tb02104.x.

[10] S. Karnik, J. Romberg, and M. A. Davenport, "Fast Multitaper Spectral Estimation," in 2019 13th International conference on Sampling Theory and Applications (SampTA), Bordeaux, France: IEEE, Jul. 2019, pp. 1–4. doi: 10.1109/SampTA45681.2019.9030939.

[11] O. Ronneberger, P. Fischer, and T. Brox, "U-Net: Convolutional Networks for Biomedical Image Segmentation," in Medical Image Computing and Computer-Assisted Intervention – MICCAI 2015, vol. 9351, N. Navab, J. Hornegger, W. M. Wells, and A. F. Frangi, Eds., in Lecture Notes in Computer Science, vol. 9351. , Cham: Springer International Publishing, 2015, pp. 234–241. doi: 10.1007/978-3-319-24574-4_28.

[12] D. Landschoot, D. Hebert, and L. Osadciw, "Real-Time Analysis of Clutter Environments for Radar Systems," in 2022 IEEE International Symposium on Phased Array Systems & Technology (PAST), Oct. 2022, pp. 1–4. doi: 10.1109/PAST49659.2022.9975049.

[13] R. S. Raghavan, "A method for estimating parameters of K-distributed clutter," IEEE Trans. Aerosp. Electron. Syst., vol. 27, no. 2, pp. 238–246, Mar. 1991, doi: 10.1109/7.78298.

[14] "Open Communications Subsystem (OCS) Standard v2.0 (U-FOUO)."

[15] "Open Mission Systems (OMS) Definition and Documentation (D&D) OMS Standard Version 1.4(U-FOUO)"

[16] D. Y. Kim, B. Ristic, R. Guan, and L. Rosenberg, "A Bernoulli trackbefore-detect filter for interacting targets in maritime radar," IEEE Trans. Aerosp. Electron. Syst., vol. 57, no. 3, pp. 1981–1991, 2021.

[17] S. Li, W. Yi, R. Hoseinnezhad, B. Wang, and L. Kong, "Multi-object tracking for generic observation model using labeled random finite sets," IEEE Trans. Signal Process., vol. 66, no. 2, pp. 368–383, 2017.

[18] Trezza, A. Murray, A. Y. Rothschild, L. Rosenberg, D. J. Bucci Jr., and P. Varshney, "Track-Before-Detect Adaptive Birth Using Generic Observation Model Labeled Random Finite Sets," accepted to IEEE Int'l Radar Conf. 2023